protein structure communications

A high-resolution structure of ligand-free human glutamate carboxypeptidase II

Cyril Barinka,[a]__*__ **Jana Starkova,**[b]
Jan Konvalinka[b,c] **and Jacek
Lubkowski**[a]

[a]National Cancer Institute at Frederick, Center
for Cancer Research, Frederick, MD 21702,
USA, [b]Gilead Sciences and IOCB Research
Centre, Institute of Organic Chemistry and
Biochemistry, Academy of Sciences of the Czech
Republic, Flemingovo n. 2, 166 10 Praha 6,
Czech Republic, and [c]Department of
Biochemistry, Faculty of Natural Science,
Charles University, Hlavova 2030, Prague,
Czech Republic

Correspondence e-mail: cyril@ncifcrf.gov

Human glutamate carboxypeptidase II (GCPII; EC 3.4.17.21) is an established
marker for prostate-cancer diagnosis as well as a candidate therapeutic target
for the treatment of diverse pathologies that involve glutamatergic transmission.
Structural data on GCPII are thus valuable for the design and optimization of
GCPII-specific inhibitors and diagnostic probes. The currently available
structure of ligand-free GCPII was refined to a resolution of 3.5 Å. This work
reports the structure of the protein refined to 1.65 Å resolution, with
crystallographic values of $R = 0.207$ and $R_{free} = 0.228$. The new structure
extends the resolution appreciably and the new model based on this data shows
significant differences when compared with the previously published model.

1. Introduction

Human glutamate carboxypeptidase II (GCPII) is a type II mem-
brane glycoprotein with an approximate molecular weight of 90–
100 kDa. The mature full-length protein consists of 750 amino-acid
residues. A short N-terminal fragment (residues 1–19), located in the
cytoplasm, is followed by a single transmembrane segment and the
707-amino-acid ectodomain, which faces the extracellular milieu.
GCPII is a homodimeric metallopeptidase that utilizes two zinc ions
to cleave a C-terminal residue from peptidic substrates (Rawlings &
Barrett, 1997). The only recognized natural substrates of GCPII to
date are *N*-acetyl-aspartyl-glutamate (NAAG) and folyl-poly-
γ-glutamates; *i.e.* peptides harboring glutamate at the C-terminus
(Pinto *et al.*, 1996; Robinson *et al.*, 1987).

In healthy individuals, GCPII is expressed predominantly in the
central nervous system and on the brush-border membrane of the
proximal small intestine (Šácha *et al.*, 2007; Troyer *et al.*, 1995). In the
latter compartment GCPII participates in the absorption of dietary
folates (Halsted *et al.*, 1998), while the neural form of the enzyme
modulates neurotransmission by NAAG hydrolysis and the conco-
mitant glutamate release (Robinson *et al.*, 1987). Inhibition of GCPII
peptidase activity showed efficacy under pathological conditions
associated with dysregulated glutamatergic transmission, such as in
experimental models of pain, brain injury or amyotrophic lateral
sclerosis (for a recent review, see Neale *et al.*, 2005 and references
therein). Since GCPII expression is highly upregulated in the
neovasculature of solid tumors as well as in prostate cancer (Bostwick
et al., 1998), the enzyme is an obvious target for the treatment and
imaging of these malignancies (Gao *et al.*, 1997). Consequently,
potent and selective small-molecule inhibitors or functionalized
ligands of the enzyme are being developed and tested in preclinical
settings (Zhou *et al.*, 2005 and references therein).

The recently reported crystal structures of the human GCPII
ectodomain in complex with glutamate, phosphate and GPI-18431
(PDB codes 2c6g, 2c6p and 2c6c, respectively) have revealed the
presence of three GCPII subdomains, protease-like (residues 57–116
and 352–590), apical (residues 117–351) and C-terminal (residues
591–750), and it was noted that cooperation between all three
subdomains is required for efficient substrate binding and hydrolysis.
Furthermore, detailed analysis of the structures led to the hypothesis
of an induced-fit mechanism of substrate recognition by GCPII, in

Table 1

Data-collection and refinement statistics.

Values in parentheses are for the highest resolution shell.

Data-collection statistics	
Wavelength (Å)	1.000
Space group	$I222$
Unit-cell parameters (Å)	$a = 101.76$, $b = 130.13$, $c = 158.87$
Resolution limits (Å)	30.0–1.65 (1.71–1.65)
No. of unique reflections	126082 (11591)
Redundancy	9.8 (6.5)
Completeness (%)	98.7 (91.6)
$I/\sigma(I)$	19.7 (2.6)
R_{merge}	0.082 (0.598)
Refinement statistics	
Resolution limits (Å)	30.0–1.65 (1.69–1.65)
Total No. of reflections	124511 (8917)
No. of reflections in working set	118244 (8477)
No. of reflections in test set	6267 (440)
R	0.207 (0.293)
R_{free}	0.228 (0.311)
Total No. of non-H atoms	6511
No. of non-H protein atoms	5946
No. of ions	4
No. of water molecules	561
Average B factor for all atoms (Å^2)	29.3
Average B factor for protein atoms (Å^2)	27.9
Ramachandran plot (%)	
Most favored	89.2
Additionally allowed	10.3
Generously allowed	0.3
Disallowed	0.2 [Lys207]
R.m.s. deviations	
Bond lengths (Å)	0.019
Bond angles (°)	1.79
Planarity (Å)	0.009
Chiral centers (Å^3)	0.12

which the $\beta15/\beta16$ hairpin (residues 692–704; termed the 'glutarate sensor') probes the S1′ pocket for the presence or absence of glutamate (Mesters *et al.*, 2006). In addition to the above-mentioned moderate-resolution X-ray structures of GCPII complexes, Davis and coworkers also published the X-ray structure of ligand-free GCPII (GCPII$_{old}$; PDB code 1z8l) refined to 3.5 Å resolution (Davis *et al.*, 2005).

Therefore, a ligand-free structure of recombinant human GCPII (rhGCPII$_{new}$) refined at a resolution of 1.65 Å and reported here represents a marked improvement in the quality of the model and allows the accurate description of the GCPII active site in the absence of ligands. This information will be significant in the elucidation of the mechanism of substrate hydrolysis by human GCPII and will permit the description of the conformational changes accompanying substrate/inhibitor binding.

2. Materials and methods

2.1. Expression and purification of rhGCPII

An extracellular part of human GCPII (rhGCPII$_{new}$; amino acids 44–750) was heterologously overexpressed in *Drosophila* Schneider S2 cells and purified to homogeneity as described previously (Barinka *et al.*, 2002). Briefly, the recombinant protein was purified from conditioned medium by a succession of ion-exchange, affinity and size-exclusion chromatographies. The final protein preparation was >97% pure, as determined by Coomassie-staining SDS–PAGE (data not shown). The protein was extensively dialyzed against 100 mM NaCl, 20 mM Tris–HCl pH 8.0, concentrated to 10 mg ml^{-1} and stored at 193 K.

2.2. Crystallization and diffraction data collection

Initial crystallization screening was performed using a Hydra II robot (Apogent Discoveries, Hudson, USA) and a sitting-drop vapor-diffusion setup, with the rhGCPII at concentration of 10 mg ml^{-1}. The final crystallization solution was composed of 33%(v/v) pentaerythritol propoxylate PO/OH 5/4, 1–3%(w/v) PEG 3350 and 100 mM Tris–HCl pH 8.0. For data collection, rhGCPII crystals were grown in hanging drops formed by mixing equal volumes of the protein and crystallization solutions. 2 µl drops were equilibrated against 1 ml reservoir solution at 293 K and crystals of approximate dimensions 0.5 × 0.5 × 0.2 mm grew within several weeks. Prior to X-ray exposure, crystals taken directly from the drop were cryo-preserved in liquid nitrogen. The diffraction pattern was collected from a single crystal at the SER-CAT beamline (sector 22-BM) at the Advanced Photon Source (Argonne, Illinois, USA) equipped with a MAR Research CCD detector using a 1.000 Å wavelength. The measurements were conducted at 100 K. All data were integrated and scaled with the *HKL*-2000 program suite (Otwinowski & Minor, 1997) and the appropriate X-ray data statistics are summarized in Table 1.

2.3. Structure determination and refinement

Because of the identical symmetry and very similar unit-cell parameters of the rhGCPII–glutamate (PDB code 2c6g) and rhGCPII$_{new}$ crystals, the structure solution was limited to rigid-body refinement of the rhGCPII–glutamate model (without water molecules and the S1′-bound glutamate) against the rhGCPII$_{new}$ diffraction intensities. This procedure, which was conducted at 2.5 Å resolution, was followed by the refinement of atomic coordinates and B factors with a gradual extension of the resolution to the limit of the experimental data (1.65 Å). Calculations were performed with the program *REFMAC* v.5.1 (Murshudov *et al.*, 1999). The refinement protocol was interspersed with manual corrections to the model using the computer-graphics program *O* (Jones *et al.*, 1991). During the refinement, a randomly selected 5% of the reflections were kept aside for cross-validation (R_{free}). The final values of the R factor and R_{free} were 0.207 and 0.228, respectively, for data in the resolution range 30–1.65 Å. Detailed statistics for the refined structure are given in Table 1.

3. Results and discussion

3.1. Screening and crystallization

The main problem limiting the resolution of the previously reported structures of GCPII was the lack of suitable conditions for freezing the crystals prior to X-ray exposure. To address this issue, we revised the crystallization conditions for rhGCPII using several crystallization screens from commercial sources. The final selection of a mother liquor composed of 33%(v/v) pentaerythritol propoxylate (5/4 PO/OH; Hampton Research) and 100 mM Tris–HCl pH 8.0 was suggested by the results of crystallization from reagent No. 56 in Index Screen (Hampton Research). The addition of 1–3%(w/v) PEG 3350 increased the probability of crystal nucleation and accelerated the rate of crystal growth. Under the newly established conditions, rhGCPII$_{new}$ crystallizes in the orthorhombic space group $I222$, with one molecule per asymmetric unit and unit-cell parameters $a = 101.76$, $b = 130.13$, $c = 158.87$ Å. This crystal form is virtually identical to the previously reported crystal forms of the GCPII complexes (Mesters *et al.*, 2006), but the presence of 5/4 PO/OH as the primary crystallization and cryoprotectant agent (Gulick *et al.*, 2002) allowed the

protein structure communications

cryopreservation of rhGCPII$_{new}$ crystals for experiments without a visible loss in diffraction quality. It should be noted that the recently published structure of ligand-free GCPII$_{old}$ was crystallized in space group $P2_1$, which is different from both the crystal form presented here and the crystal forms of the above-mentioned rhGCPII complexes.

3.2. Overall structure

The 1.65 Å model of ligand-free rhGCPII$_{new}$ consists of 5946 non-H protein atoms (686 amino-acid residues), 561 water O atoms, one Ca^{2+} ion, one Cl^- ion and two Zn^{2+} ions. Most of the protein residues are well defined in the electron-density peaks. The exceptions are the first 13 N-terminal residues and a flexible loop (541–547), which could not be modeled owing to the lack of corresponding electron-density data. Since these fragments do not interact with neighboring molecules, their high flexibility is probably a property native to rhGCPII. The only other fragment not modeled in the rhGCPII$_{new}$ structure is the short (654–656) loop that directly interacts with an equivalent fragment from a symmetry-related molecule. Despite strong positive $F_o - F_c$ peaks, we were unable to deconvolve the alternate conformations for this fragment. Two alternate conformations were modeled for the side chains of 34 residues, based on the $F_o - F_c$ electron-density peaks. Unless the intensities of these peaks clearly indicated otherwise, equal occupancies were assumed for the alternate conformations. Additionally, two partially occupied main-chain conformations were evident for the protein segment 692–704. The conformational adaptability of this fragment has been suggested as being important for substrate recognition and/or binding (Mesters *et al.*, 2006). The Ramachandran analysis of the final model using the program *PROCHECK* (Laskowski *et al.*, 1993) classifies 89.2% of the residues as having the most favorable conformations,

with 10.6% of the residues adopting allowed conformations. Despite being clearly defined by the electron-density maps, Lys207 adopts a conformation that is disallowed by Ramachandran analysis.

A comparison of the resulting structure with the previously reported 3.5 Å structure of ligand-free GCPII$_{old}$ reveals the structures to be fairly similar, with an r.m.s. deviation between the 685 equivalent C^α atoms of 1.23 Å. Likewise, the overall fold of ligand-free rhGCPII$_{new}$ is almost indistinguishable from the structures of rhGCPII complexed with reaction products/inhibitors.

3.3. The active site

Two zinc ions located in the active site of rhGCPII$_{new}$ are bridged by the β-carboxylate of Asp387 and are further coordinated by the side chains of His377, Asp453, Glu425 and His553. In the structure of rhGCPII$_{new}$, an activated water molecule (or OH^-) is located symmetrically between the two Zn^{2+} ions at distances of 2.03 and 2.01 Å. This water molecule plays a central role in the hydrolysis of a substrate and is hydrogen bonded to the conserved Glu424 residue ($O \cdots OE1$, 2.92 Å) that functions as a proton shuttle during scissile bond cleavage. A similar arrangement of the active site has been reported previously for the ligand-free GCPII$_{old}$, although the interatomic distances between the activated water and Glu424 γ-carboxylate were too long ($\sim$3.8 Å) for efficient proton transfer (Davis *et al.*, 2005).

3.4. The substrate-binding cavity

The S1′ pocket of GCPII is defined by residues Phe209, Arg210, Asn257, Gly427, Leu428, Gly518, Lys699 and Tyr700. The latter two are part of a flexible 'glutarate sensor' (Mesters *et al.*, 2006). The positions of most of the residues lining the S1′ pocket are similar in the GCPII$_{old}$ and rhGCPII$_{new}$ structures. The exceptions are the amino acids from the glutarate sensor (Lys699 and Tyr700) and the side chain of Phe209. The Phe209 side chain is rotated by $\sim$120° between rhGCPII$_{new}$ and GCPII$_{old}$, resulting in a shift of $\sim$8 Å between the CZ atoms of the two models. The different conformation of Phe209 in GCPII$_{old}$ might reflect a natural positional flexibility of this residue; however, Phe209 adopts an invariable conformation (as observed in rhGCPII$_{new}$) in all other reported structures of GCPII.

The S1′ pocket in rhGCPII$_{new}$ is occupied by a network of six water molecules. Four of these molecules (one in two alternate positions) occupy the approximate positions of the N, OXT, CB, OE1 and OE2 atoms of a glutamate ligand in the rhGCPII–glutamate complex (Mesters *et al.*, 2006), while the fifth water is conserved in both the complex and rhGCPII$_{new}$. The sixth water forms hydrogen bonds to Tyr552 OH (2.62 Å) and His553 NE2 (3.09 Å) and coordinates the Zn^{2+} ion at 2.48 Å.

The bottom of the S1′ pocket is closed by a flexible loop formed by residues 692–704 (the 'glutarate sensor'). Two residues from this loop (Lys699 and Tyr700) interact directly with a C-terminal residue of a substrate in the GCPII complexes and the glutarate sensor can adopt various conformations, largely depending on the occupancy of the S1′ pocket (Mesters *et al.*, 2006; Davis *et al.*, 2005). Two conformations of the glutarate sensor were modeled in the rhGCPII$_{new}$ structure, with a maximal positional difference of $\sim$6 Å (C^α atoms of Gly702). An ensemble of the variable conformations of the glutarate sensor is shown in Fig. 1, where the published structures of GCPII are superimposed on the model of rhGCPII$_{new}$.

The putative S1 pocket is defined by residues Ser454, Glu457, Asp465, Asn519, Gly548, Tyr549 and Tyr552, as well as by a stack of three arginines (Arg463, Arg534 and Arg536). This positively charged arginine stack, located 6.5–12.7 Å from the nearest Zn^{2+} ion,
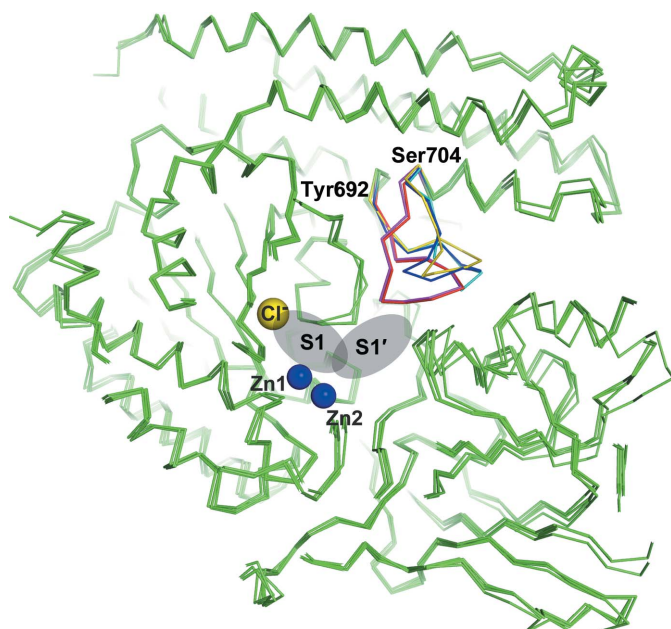

Figure 1
Ensemble of conformations of the 'glutarate sensor'. Two residues in this segment, Lys699 and Tyr700, interact directly with the ligands of the S1′ site. The GCPII structures available from the PDB were superimposed on the structure of rhGCPII$_{new}$. The C^α traces are shown in ribbon representation, the active-site Zn^{+2} ions are shown as blue spheres and the yellow sphere represents the S1-bound Cl^- ion. The 'glutarate sensor' is shown in yellow for PDB entry 1z8l, in magenta for 2c6g, in blue for 2c6p and in red and cyan for the two conformations in rhGCPII$_{new}$. The S1 and S1′ sites are highlighted by gray ellipses.
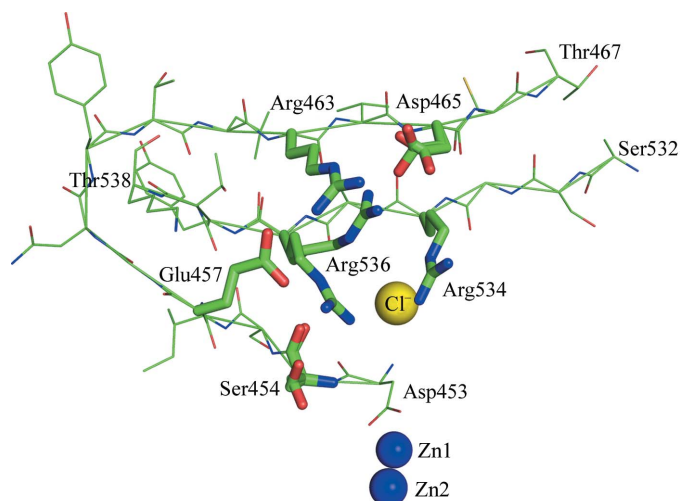
Figure 2
Organization of the positively charged arginine stack in the putative S1 pocket. Arg463, Arg534 and Arg536 are located within the antiparallel β-strands (β14, Ser532–Thr538; β13, Thr461–Cys466). In the rhGCPII$_{new}$ structure, Arg463 and Arg534 are present in single conformations, while Arg536 adopts two alternate conformations. The S1-bound Cl$^-$ ion (shown as a yellow sphere) stabilizes the invariant conformation of Arg534 as well as neutralizing the positive charge contributed by the Arg534 and Arg536 guanidinium groups. The side chains of Ser454, Asp465 and Arg536 are shown in two alternate conformations and the active-site Zn^{+2} ions are represented as blue spheres.

is believed to be responsible for the enzyme's preference for negatively charged residues in the penultimate (*i.e.* P1) position of a substrate (Barinka *et al.*, 2002; Mesters *et al.*, 2006). The invariant positions of the guanidinium groups in Arg534 and Arg463 are maintained by interaction with a Cl$^-$ ion and a strong hydrogen bond (2.59 Å) to the γ-carboxylate of Glu457, respectively. The side chain of Arg536 adopts two conformations. In the slightly more abundant conformation, the guanidinium group of Arg536 forms two hydrogen bonds to Ser454 OG (NH1$\cdots$OG, 3.21 Å; NH2$\cdots$OG, 3.24 Å) and one to Ser454 O (3.03 Å), Glu457 OE1 (2.85 Å) and Cl$^-$ (3.26 Å) (Fig. 2). Thus, the role of the Cl$^-$ ion is in stabilizing the positions of Arg534 and Arg536 and in neutralizing the combined positive charge of their guanidinium groups. It has been suggested that the chloride ion is essential for GCPII hydrolytic activity (Robinson *et al.*, 1987). In the less occupied conformation, the stabilization of the guanidinium group of Arg536 provided by stacking between Arg463 and Arg534 is further stabilized by ionic interactions with the negatively charged carboxylate of Asp465.

4. Conclusions

In summary, our newly established crystallization conditions allowed us to determine and refine the structure of ligand-free rhGCPII$_{new}$ at a resolution of 1.65 Å. A comparison with the GCPII$_{old}$ model reveals several marked differences in the organization of the substrate-binding cavity of this enzyme. Thus, the present structure could serve as a more accurate model for ensuing biochemical/structural studies.

References

Barinka, C., Rinnova, M., Sacha, P., Rojas, C., Majer, P., Slusher, B. S. & Konvalinka, J. (2002). *J. Neurochem.* **80**, 477–487.
Bostwick, D. G., Pacelli, A., Blute, M., Roche, P. & Murphy, G. P. (1998). *Cancer*, **82**, 2256–2261.
Davis, M. I., Bennett, M. J., Thomas, L. M. & Bjorkman, P. J. (2005). *Proc. Natl Acad. Sci. USA*, **102**, 5981–5986.
Gao, X., Porter, A. T., Grignon, D. J., Pontes, J. E. & Honn, K. V. (1997). *Prostate*, **31**, 264–281.
Gulick, A. M., Horswill, A. R., Thoden, J. B., Escalante-Semerena, J. C. & Rayment, I. (2002). *Acta Cryst.* D**58**, 306–309.
Halsted, C. H., Ling, E. H., Luthi-Carter, R., Villanueva, J. A., Gardner, J. M. & Coyle, J. T. (1998). *J. Biol. Chem.* **273**, 20417–20424.
Jones, T. A., Zou, J.-Y., Cowan, S. W. & Kjeldgaard, M. (1991). *Acta Cryst.* A**47**, 110–119.
Laskowski, R. A., MacArthur, M. W., Moss, D. S. & Thornton, J. M. (1993). *J. Appl. Cryst.* **26**, 283–291.
Mesters, J. R., Barinka, C., Li, W., Tsukamoto, T., Majer, P., Slusher, B. S., Konvalinka, J. & Hilgenfeld, R. (2006). *EMBO J.* **25**, 1375–1384.
Murshudov, G. N., Vagin, A. A., Lebedev, A., Wilson, K. S. & Dodson, E. J. (1999). *Acta Cryst.* D**55**, 247–255.
Neale, J. H., Olszewski, R. T., Gehl, L. M., Wroblewska, B. & Bzdega, T. (2005). *Trends Pharmacol. Sci.* **26**, 477–484.
Otwinowski, Z. & Minor, W. (1997). *Methods Enzymol.* **276**, 307–326.
Pinto, J. T., Suffoletto, B. P., Berzin, T. M., Qiao, C. H., Lin, S., Tong, W. P., May, F., Mukherjee, B. & Heston, W. D. (1996). *Clin. Cancer Res.* **2**, 1445–1451.
Rawlings, N. D. & Barrett, A. J. (1997). *Biochim. Biophys. Acta*, **1339**, 247–252.
Robinson, M. B., Blakely, R. D., Couto, R. & Coyle, J. T. (1987). *J. Biol. Chem.* **262**, 14498–14506.
Šácha, P., Zámečník, J., Bařinka, C., Hlouchová, K., Vícha, A., Mlčochová, P., Hilgert, I., Eckschlager, T. & Konvalinka, J. (2007). *Neuroscience*, **144**, 1361–1372.
Troyer, J. K., Beckett, M. L. & Wright, G. L. Jr (1995). *Int. J. Cancer*, **62**, 552–558.
Zhou, J., Neale, J. H., Pomper, M. G. & Kozikowski, A. P. (2005). *Nature Rev. Drug Discov.* **4**, 1015–1026.